Fast Lean-Rich Cycling for Enhanced NO_x Conversion on Storage and Reduction Catalysts

A Thesis

Presented to

the Faculty of the Department of Chemical and Biomolecular Engineering

University of Houston

In Partial Fulfillment

of the Requirements for the Degree

Master of Science

in Chemical Engineering

by

Charles C.Y. Perng

May 2014

Fast Lean-Rich Cycling for Enhanced NO_x Conversion

on Storage and Reduction Catalysts

Charles C.Y. Perng

Approved:

Chair of the Committee
Dr. Michael P. Harold, Professor,
Chair of Chemical and Biomolecular Engineering

Committee Members:

Dr. William S. Epling, Associate Professor,
Chemical and Biomolecular Engineering

Dr. Matthew A. Franchek, Professor,
Director of Subsea Engineering Program,
Mechanical Engineering

Dr. Suresh K. Khator, Associate Dean,
Chair of Cullen College of Engineering

Dr. Michael P. Harold, Professor,
Chair of Chemical and Biomolecular Engineering

Acknowledgements

First and foremost, I would like to thank Dr. Michael Harold for the support, encouragement, and direction he has given me throughout this endeavor. I would also like to express my sincere gratitude to Dr. Vencon Easterling for the contributions he has made to this work and our first publication. I would like to recognize my labmates Gregory Bugosh, Dr. Prasanna Dasari, Mengmeng Li, and all other members of the TxCEF team for helping me get started and providing suggestions throughout the process. I owe special thanks to BASF for providing the model catalysts used in this study and the Department of Energy for funding this research.

Fast Lean-Rich Cycling for Enhanced NO_x Conversion on Storage and Reduction Catalysts

An Abstract

of a

Thesis

Presented to

the Faculty of the Department of Chemical and Biomolecular Engineering

University of Houston

In Partial Fulfillment

of the Requirements for the Degree

Master of Science

in Chemical Engineering

by

Charles C.Y. Perng

May 2014

Abstract

Lean NO_x ($NO + NO_2$) reduction was carried out using rapid periodic injection of C_3H_6 over a NO_x storage and reduction (NSR) monolith catalyst containing $Pt/Rh/BaO/CeO_2/Al_2O_3$. The effects of injection speed, feed temperature, rich phase composition, lean phase duration, and feed concentration of CO_2 were systematically studied to highlight distinct performance characteristics at faster injection frequencies. Increased NO_x and C_3H_6 conversions were achieved using high frequency injection. The detrimental effects of barium nitrate decomposition at high temperatures and barium carbonate formation were also found to be less significant using rapid pulsing. In addition, a prolonged approach to cyclic steady state was observed for high frequency operation. The results are indicative of a qualitative mechanistic change and suggest the generation of reactive "$HC_xN_yO_z$" intermediate species that enable improved performance over traditional NSR cycling.

Table of Contents

Acknowledgements ……... iv

Abstract ……. vi

Table of Contents ……. vii

List of Figures ……. viii

List of Tables …… xi

Chapter 1. Introduction …….. 1

Chapter 2. Experimental Description ……. 7

Chapter 3. Results and Discussion ……... 10

3.1 Instantaneous Catalyst Temperature and Species Concentrations ……... 10

3.2 Cycle-Averaged Performance Trends …….. 13

3.2.1 Injection Frequency ……. 13

3.2.2 Thermal Durability …….. 19

3.2.3 Rich Phase Composition ……..21

3.2.4 Lean Phase Duration ……....23

3.2.5 Impact of CO_2 ……. 25

3.3 Transient Approach to Cyclic Steady State ……. 27

3.4 Phenomenological Mechanism …… 29

Chapter 4. Conclusions ……32

Chapter 5. Future Work …… 34

5.1 Process Optimization ……..... 34

5.2 Reaction Mechanism …… 34

5.3 Development of a Model …….. 36

References …… 38

List of Figures

Fig. 1: Schematic of the reactor and analyzer system. ……... 7

Fig. 2. Effluent NO_x/O_2 concentration and catalyst temperature for a set of typical cycling experiments, with the corresponding propylene injection patterns shown in the bottom row of the figure. Rich duty cycle and C_3H_6 concentration during the rich pulse are fixed at 14.3% and 1.75%, respectively. Feed stream contains 5% O_2 and 500 ppm NO at 275°C. Injection patterns for each column are as follows: a) 60 s lean/10 s rich (0.014 Hz). b) 12 s lean/2 s rich (0.07 Hz). c) 6 s lean/1 s rich (0.14 Hz). d) 3 s lean/0.5 s rich (0.29 Hz). …….. 10

Fig. 3. Cycle-averaged concentrations as a function of injection frequency. Feed temperature is 260°C. Flow composition is 5% O_2 and 800 ppm NO. Rich phase C_3H_6 is 2.03% (S_N = 3.9). The injection frequencies are 0.014 Hz, 0.036 Hz, 0.07 Hz and 0.14 Hz. a) Cycle-averaged NO, NO_2, N_2O and NH_3 concentrations in the effluent stream. b) Cycle-averaged C_3H_6, CO, CO_2 and H_2O concentrations in the effluent stream. c) NO_x and C_3H_6 conversion data. d) N_2, N_2O and NH_3 selectivity with cycle-averaged catalyst temperature. …….. 14

Fig. 4. NO_x and C_3H_6 conversion as a function of injection frequency at constant cycle-averaged catalyst temperature. Flow composition is 5% O_2, 10% CO_2 and 700 ppm NO. The rich phase C_3H_6 concentration is 1.9%. The feed temperature is adjusted to maintain a near constant-averaged catalyst temperature of 410°C ± 10°C. The injection frequencies are 0.014 Hz, 0.036 Hz, 0.07 Hz and 0.14 Hz. …… 16

Fig. 5. NO_x conversion and catalyst temperature as a function of injection frequency, for three cycle-averaged C_3H_6 feed concentrations. Feed temperature is 275°C. Flow composition is 5% O_2 and 500 ppm NO. The injection frequencies are 0.014 Hz, 0.07 Hz, 0.14 Hz and 0.29 Hz. a) Cycle-averaged NO_x conversion as a function of injection frequency. b) Cycle-averaged catalyst temperature as a function of injection frequency. ……... 17

Fig. 6. NO_x conversion as a function of injection frequency, for three cycle-averaged H_2 feed concentrations. Feed temperature is 275°C. Flow composition is 3% O_2 and 650 ppm NO. The injection frequencies are 0.014 Hz, 0.07 Hz, 0.14 Hz and 0.29 Hz. ……. 19

Fig. 7. Cycle-averaged NO_x conversion and catalyst temperature vs. feed temperature for two different frequencies. Flow composition is 5% O_2 and 700 ppm NO. The rich phase contains 1.75% C_3H_6. The injection patterns are 6 s lean/1 s rich (0.14 Hz) and 60 s lean / 10 s rich (0.014 Hz). ……. 20

Fig. 8. Cycled-averaged NO_x and C_3H_6 conversions verses rich phase propylene feed concentration. Lean phase C_3H_6 concentration is adjusted to maintain a cycle-averaged C_3H_6 concentration of 0.29% (S_N=3.9). Feed temperature is 250°C. Flow composition is 5% O_2 and 550 ppm NO. a) Conversions using a 60 s lean / 10 s rich (0.014 Hz) cycling pattern. b) Conversions using a 6 s lean / 1 s rich (0.14 Hz) cycling pattern. …….. 22

Fig. 9. Cycle-averaged concentrations as a function of lean phase length. Feed temperature is 300°C. Flow composition is 5% O_2 and 600 ppm NO. Rich phase C_3H_6 is 1.9% ($S_{N,p}$ = 0.6) and rich pulse duration is 0.5 s. Total cycle length and S_N varies. a) Cycle-averaged NO, NO_2, N_2O and NH_3 concentrations in the effluent stream. b) Cycle-

averaged C_3H_6, CO, CO_2 and H_2O concentrations in the effluent stream. c) NO_x and C_3H_6 conversion data with corresponding average S_N. d) N_2, N_2O and NH_3 selectivity with cycled-averaged catalyst temperature. ……. 24

Fig. 10. Effect of CO_2 on NO_x conversion for varying frequencies. Flow composition is 5% O_2, 550 ppm NO, and 0% ( ) or 10% ( ) CO_2. Rich phase C_3H_6 is 2.2%. a) NO_x conversion at T_f = 250°C. b) NO_x conversion at T_f = 375°C. c) Decrease in NO_x conversion due to the addition of 10% CO_2 at T_f = 250°C and T_f = 375°C. …….. 26

Fig. 11: Transient NO_x released in the effluent as the reactor transitions from lean conditions with NO_x initially stored on the catalyst to periodic steady state cycling conditions. Feed composition is 5% O_2, 10% CO_2, 700 ppm NO and rich phase C_3H_6 = 1.9%. The feed temperature is adjusted to maintain a near constant cycle-averaged catalyst temperature (Avg. T_c = 410°C ± 10°C). Cycling begins at t=0 s. a) Transient NO_x concentration. b) Moving average of transient NO_x concentration, averaged over 1 cycle length. c) Moles of NO_x released in the effluent and average catalyst temperature. d) Time required for NO_x averaged over 1 cycle to reach 95% of the periodic steady state cycle-averaged NO_x concentration value. ……..... 28

List of Tables

Table 1: U.S. Tier 2 Emission Standards, FTP 75, g/mi …… 1

Table 2: E.U. Emission Standards for Passenger Cars (Category M_1) …….. 2

Chapter 1. Introduction

Increased awareness of the environmental and health implications of air pollutants has led to the development of more stringent government regulations. These mandates account for the emission of NO_x, CO, and hydrocarbons (HCs) from vehicle exhaust, as well as greenhouse gases such as CO_2. Table 1 and Table 2 show pollutant emission standards (adapted from DieselNet) for the United States [1] and European Union [2], respectively. The current U.S. Tier 2, Bin 5 emission standard (fully implemented in 2009) for NO_x is 0.05 g/mi, while the current E.U. emission standard for NO_x in diesel passenger vehicles is 0.18 g/km.

Table 1: U.S. Tier 2 Emission Standards, Federal Test Procedure 75, g/mi

Bin #	**Intermediate life (5 years / 50,000 mi)**					**Full useful life (10 years/ 120,000 mi)**				
	NMOG*	**CO**	**NO_x**	**PM†**	**HCHO**	**NMOG***	**CO**	**NO_x**	**PM†**	**HCHO**
Temporary Bins										
11						0.28	7.3	0.9	0.1	0.032
10	0.125 (0.160)	3.4 (4.4)	0.4	-	0.015 (0.018)	0.156 (0.230)	4.2 (6.4)	0.6	0.1	0.018 (0.027)
9	0.075 (0.140)	3.4	0.2	-	0.015	0.090 (0.180)	4.2	0.3	0.1	0.018
Permanent Bins										
8	0.100 (0.125)	3.4	0.14	-	0.015	0.125 (0.156)	4.2	0.2	0	0.018
7	0.075	3.4	0.11	-	0.015	0.09	4.2	0.15	0	0.018
6	0.075	3.4	0.08	-	0.015	0.09	4.2	0.1	0	0.018
5	0.075	3.4	0.05	-	0.015	0.09	4.2	0.07	0	0.018
4	-	-	-	-	-	0.07	2.1	0.04	0	0.011
3	-	-	-	-	-	0.055	2.1	0.03	0	0.011
2	-	-	-	-	-	0.01	2.1	0.02	0	0.004
1	-	-	-	-	-	0	0	0	0	0

* NMOG (non-methane organic gases) means NMHC (non-methane hydrocarbons) for diesel vehicles
† PM (particulate matter)
Pollutants with two numbers have a certification standard (1st number) and in-use standard (2nd number)

Table 2: E.U. Emission Standards for Passenger Cars (Category M_1)

Stage	Date	CO	HC	HC+NO_x	NO_x	PM	PN
		g/km					#/km
Compression Ignition (Diesel)							
Euro 1	1992.07	2.72 (3.16)	-	0.97 (1.13)	-	0.14 (0.18)	-
Euro 2, IDI*	1996.01	1	-	0.7	-	0.08	-
Euro 2, DI*	1996.01	1	-	0.9	-	0.1	-
Euro 3	2000.01	0.64	-	0.56	0.5	0.05	-
Euro 4	2005.01	0.5	-	0.3	0.25	0.025	-
Euro 5a	2009.09	0.5	-	0.23	0.18	0.005	-
Euro 5b	2011.09	0.5	-	0.23	0.18	0.005	6.0×10^{11}
Euro 6	2014.09	0.5	-	0.17	0.08	0.005	6.0×10^{11}
Positive Ignition (Gasoline)							
Euro 1	1992.07	2.72 (3.16)	-	0.97 (1.13)	-	-	-
Euro 2	1996.01	2.2	-	0.5	-	-	-
Euro 3	2000.01	2.3	0.2	-	0.15	-	-
Euro 4	2005.01	1	0.1	-	0.08	-	-
Euro 5	2009.09	1	0.1	-	0.06	0.005	-
Euro 6	2014.09	1	0.1	-	0.06	0.005	6.0×10^{11}

* DI (direct injection) and IDI (indirect injection) diesel engines
† PN (particle number)

Lean burn gasoline and diesel vehicles operate in oxygen excess conditions, which results in increased fuel efficiency and reduced CO_2 emissions. However, excess oxygen in the exhaust undermines the effectiveness of the conventional three-way catalytic converter in reducing NO_x to N_2. Thus, the mandate to reduce diesel engine NO_x emissions creates a challenge in the treatment of emissions from lean burn vehicles. One of the earliest responses to this challenge was the development of the NO_x storage and reduction (NSR) process by Toyota researchers in the mid 1990's [3,4]. NSR involves deliberate lean-rich cycling over a bifunctional catalyst to achieve higher NO_x conversion. During the lean phase (in which excess oxygen is present), NO is oxidized to NO_2 on the precious metal function (e.g., Pt, Rh) and subsequently stored on the storage

function (e.g., BaO, CeO_2) in the form of nitrite and nitrate species. During the oxygen deficient rich phase, a reductant (e.g., H_2, CO, hydrocarbons) is introduced into the exhaust, which leads to the release of stored NO_x species and their subsequent reduction to N_2 on the precious metal sites [4,5].

Numerous studies have been conducted with the goal of identifying the catalytic properties and operating conditions that achieve high NO_x conversion. Reviews of NSR catalysts were provided earlier by Epling et al. [6], and more recently by Roy and Baiker [7] and Harold [8]. Exhaust temperatures below 200^{o}C pose a particular challenge because of a combination of inadequate NO oxidation and stored NO_x regeneration activity of the NSR catalyst. On the other hand, at high temperatures (>400^{o}C), the thermodynamic stability of stored nitrates decreases so that the high NO_x reduction rate cannot be fully exploited. As a result of these limiting behaviors, a maximum in the cycle-averaged NO_x conversion is achieved at intermediate temperatures (300 – 350^{o}C) [6,9–11]. Another challenge is the unwanted release of NO/NO_2 at the initial stages of the regeneration, the so-called "NO_x puff". NO_x is released due to the shift in the gas phase composition. This leads to the decomposition of nitrites/nitrates, further exasperated by exotherms associated with rich mixtures containing O_2. When the amount of reductant is insufficient to react with the released NO_x, a spike in the effluent NO_x is observed [6,12]. The puff can be mitigated by careful manipulation of the cycle timing and regeneration conditions [13]. Complicating the situation is the production of undesired NO_x reduction byproducts such as N_2O and NH_3, which are typically more problematic at lower temperatures [10,14]. The selectivity of these unwanted byproducts has been explained by a moving front concept by multiple groups [11,15–22].

Process parameters can have a significant effect on lean NO_x trap (LNT) performance. These include the cycle timing and feed composition. Intermediate values for total cycle length and rich duty cycle were shown by Kabin et al. [10] to achieve a maximum NO_x conversion, with the optimum values depending on flow conditions. Muncrief et al. [23] determined that short pulses of high concentration achieve a higher NO_x conversion than longer pulses of reduced concentration. The dynamic storage capacity, which represents the amount of NO_x stored prior to NO_x breakthrough, was also reported to achieve a maximum around 350°C. Since H_2O and CO_2 are in large excess in vehicle exhaust, understanding their effects on LNT performance can provide some clues about the storage and reduction processes. Epling et al. [24] studied the effects of CO_2 on NO_x sorption. The presence of CO_2 was found to have a detrimental effect on both the trapping efficiency of the catalyst and the induction time before NO_x slip occurs during storage. This is attributed to the formation of Ba carbonate species, which are more thermally stable than barium oxides in forming the nitrate species. The presence of H_2O also reduces the trapping efficiency of the catalyst by eliminating NO_x adsorption on γ-Al_2O_3 sites. The effect of both CO_2 and H_2O in the feed stream is similar to CO_2 alone, and it has been proposed that carbonate species are able to displace hydroxide species.

More recent studies have led to an even more detailed understanding of NSR. Spatially-resolved measurements confirmed earlier work that NH_3 is an important intermediate which is formed upstream and consumed downstream [15,17,19,25–26]. Through the use of a fast switching apparatus and isotopically labeled nitric oxide (^{15}NO), Breen et al. [27] observed the presence of two N_2 peaks during NSR cycling

experiments. The first N_2 peak was due to the reduction of stored NO_x, as the feed was switched from the lean phase to the rich phase. The second N_2 peak occurred as the feed was switched back from rich to lean conditions. One explanation proposed by the authors for the second N_2 peak is the reaction between gas phase NO_x and NH_3 formed from the hydrolysis of isocyanates on the catalyst surface. Dasari and Harold [28] have added new insight on the role of the isocyanate mechanism during NSR.

Expanding upon the discovery of this second N_2 peak, researchers at the Toyota Motor Corporation have developed a high performance deNO_x system, given the name "Diesel NO_x aftertreatment by Adsorbed Intermediate Reductants" (Di-Air) [29]. The Di-Air method utilizes rapid periodic injection of hydrocarbons to achieve enhanced performance over traditional NSR. Toyota researchers reported higher NO_x conversions for a wider range of space velocities, temperatures and sulfur exposure than conventional NSR cycling. The performance enhancement was attributed to intermediates generated from the reaction between adsorbed NO_x and partially oxidized hydrocarbons produced in the front portion of the catalyst during rapid periodic injection. Through DRIFTS (*in situ* diffuse reflectance infrared Fourier transform spectroscopy) measurements, the authors assigned a peak to the intermediate surface species containing both N and C. Inoue et al. [30] further investigated the thermal stability of the intermediate species using temperature programmed desorption. The intermediates produced from C_3H_6 (represented by R-NCO and R-CN) were found to remain on the catalyst up to 600°C. It was concluded that the intermediates have a strong affinity for the NSR catalyst which enables them to remain on the catalyst surface at higher temperatures, providing an

alternative for the C_3H_6 oxidation reaction and reacting with adsorbed NO_x to produce N_2.

The current study examines the effect of rapid periodic injection of C_3H_6 on the performance of a model NSR catalyst through the systematic variation of several operating parameters. The objective is to gain a better understanding of the effects of injection frequency, to determine the generality of these effects, and to build a phenomenological mechanism with propylene as the reductant over a $Pt/Rh/BaO/CeO_2/Al_2O_3$ catalyst. Both transient concentrations and cycle-averaged performance metrics (conversion, selectivity, and catalyst temperature) are measured as a function of the reductant injection frequency. The temperature range over which high conversion of NO_x and propylene are obtained is determined, as are the effects of C_3H_6 feed composition during the rich phase and lean phase length. A proposed mechanistic picture is interpreted by examining the inhibitory effect of CO_2 and comparing propylene and hydrogen injection over a range of frequencies.

Chapter 2. Experimental Description

A schematic of the experimental apparatus is shown in Fig. 1. The monolith catalysts used in this study were provided by BASF (Iselin, NJ). The catalysts contain $Pt/Rh/BaO/CeO_2/Al_2O_3$, with specifications of 80 g Pt/ft^3 monolith, 10 g Rh/ft^3 monolith, 15 wt.% Ba (in wash coat), and 17 wt.% Ce on a γ-alumina support. Small cylindrical catalyst samples (D = 0.5 in, L = 1 in) were cut from the larger cylindrical core using a drill press equipped with a dry diamond drill bit. The catalyst was wrapped with ceramic paper to prevent gas bypass and placed in a quartz tube reactor heated by a tube furnace.

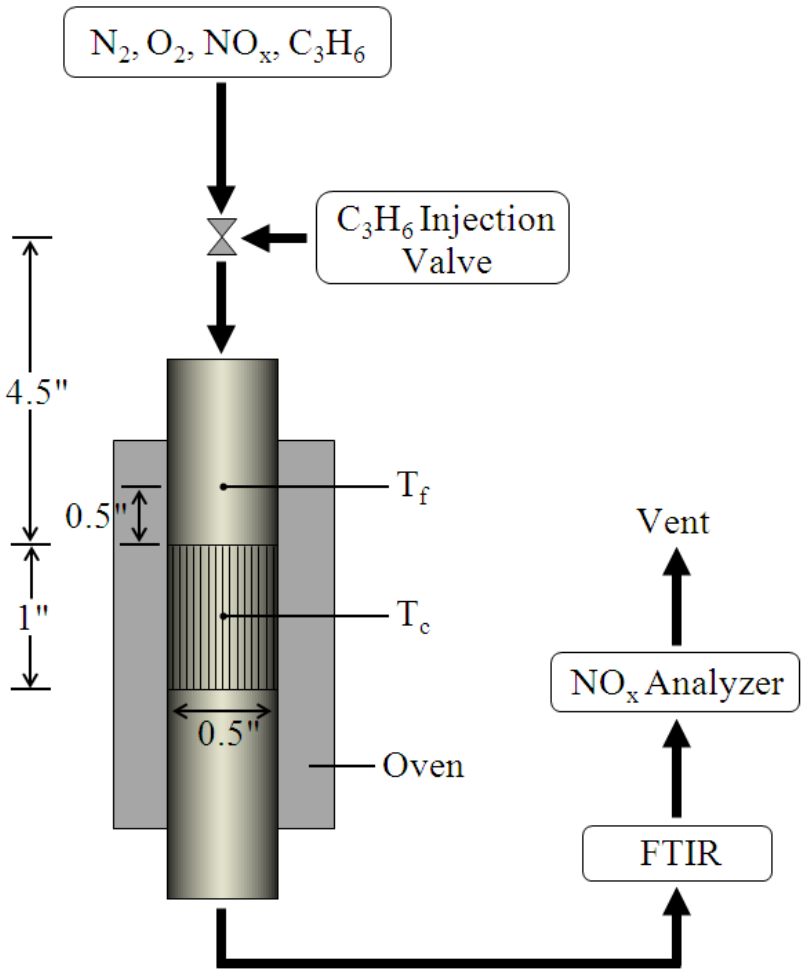

Fig. 1: Schematic of the reactor and analyzer system.

Diesel engine exhaust was simulated using cylinder-supplied gases (Praxair – UHP N_2, UHP Air, UHP CO_2, 5% NO, 99.79% C_3H_6), with the typical feed stream containing N_2, O_2, NO and C_3H_6 in a N_2 carrier gas. In all experiments, the total gas flow was 3000 cm^3/min, corresponding to a gas hourly space velocity (GHSV) of ca. 56,000 hr^{-1} at standard conditions. The feed NO concentration was in the range of 500 to 800 ppm. Rich phase C_3H_6 was injected using a high speed solenoid valve, with a specification response time of 5 ms (Parker Hannifin Corp., Series 9 – Miniature Calibrant Gas Valve). In order to minimize dispersion effects, the injection valve was placed close to the catalyst (11-12 cm upstream), but far enough away to allow the feed stream to be preheated. The distance from the point of injection and the catalyst was found to have a measureable effect on conversion. This design variable was not examined in the current study, but it will be addressed in future work. Since previous studies have shown a rich duty cycle (rich phase length divided by total cycle time) of 14.3% to achieve a maximum for NO_x conversion, this value was used for the majority of this study [10,23]. Further research will also be needed to find the optimum injection protocol for this reactor system.

Localized feed gas and catalyst temperatures were measured using two K-Type thermocouples. The temperature of the feed stream entering the reactor (T_f) was measured using a thermocouple placed 0.5 inch upstream of the catalyst. Another thermocouple was positioned in the midpoint of the monolith to measure the temperature at the center of the catalyst (T_c). It is noted that the catalyst temperature better represents the state of the catalyst, but it is a dependent variable.

The outlet gas stream flowed through a heated line at ca. 190°C to the MultiGas 2030 FTIR (MKS Instruments), which was used to measure concentrations of NO, NO_2, N_2O, C_3H_6, NH_3, CO, CO_2 and H_2O. The gas stream was then sent to a NO_x chemiluminescence detector (NOxMAT 600, Siemens) to measure total NO_x concentration ($NO+NO_2$). The injection valve, thermocouples and chemiluminescence detector were all controlled/monitored using LABVIEW software. Time delays between the system and the equipment were accounted for in the data processing.

The stoichiometric number is given as the molar ratio of oxidizing to reducing components, expressed as

$$S_N = \frac{2[O_2] + [NO]}{9[C_3H_6] + [H_2]} \ . \qquad (1)$$

A S_N greater than unity represents a lean mixture, whereas a S_N less than unity represents a rich mixture. $S_{N,p}$ and S_N denote the stoichiometric number of the feed stream during the rich pulse and the time-averaged value, respectively. Fractional NO_x and C_3H_6 conversions and product selectivities were determined with standard expressions [10]. The effluent N_2 was not directly measured, but was calculated from a nitrogen balance, assuming the N_2 carrier gas is inert. Similarly, the effluent O_2 concentration is determined from the appropriate balance on oxygen species.

Lean-rich cycling experiments were conducted to determine the effects of injection frequency, feed temperature, rich phase concentration, lean phase length and the presence of CO_2. In the case of cyclical data, the concentrations were found by averaging over complete cycles, allowing sufficient time for the system to reach a cyclic steady state.

Chapter 3. Results and Discussion

3.1 Instantaneous Catalyst Temperature and Species Concentrations

The effect of pulse injection frequency was examined for a base case operation. Fig. 2 shows the time dependence of the effluent NO_x and O_2 concentrations. Four C_3H_6 injection frequencies between 0.014 and 0.29 Hz are depicted in the bottom row of the figure, while the corresponding effluent NO_x (O_2) concentration and catalyst temperature are shown in the top (middle) row of the figure. The duty cycle was fixed at 14.3% for all four injection frequencies. From left to right in the figure, the injection patterns are: 60 s lean/10 s rich (0.014 Hz), 12 s lean/2 s rich (0.07 Hz), 6 s lean/1 s rich (0.14 Hz) and 3 s

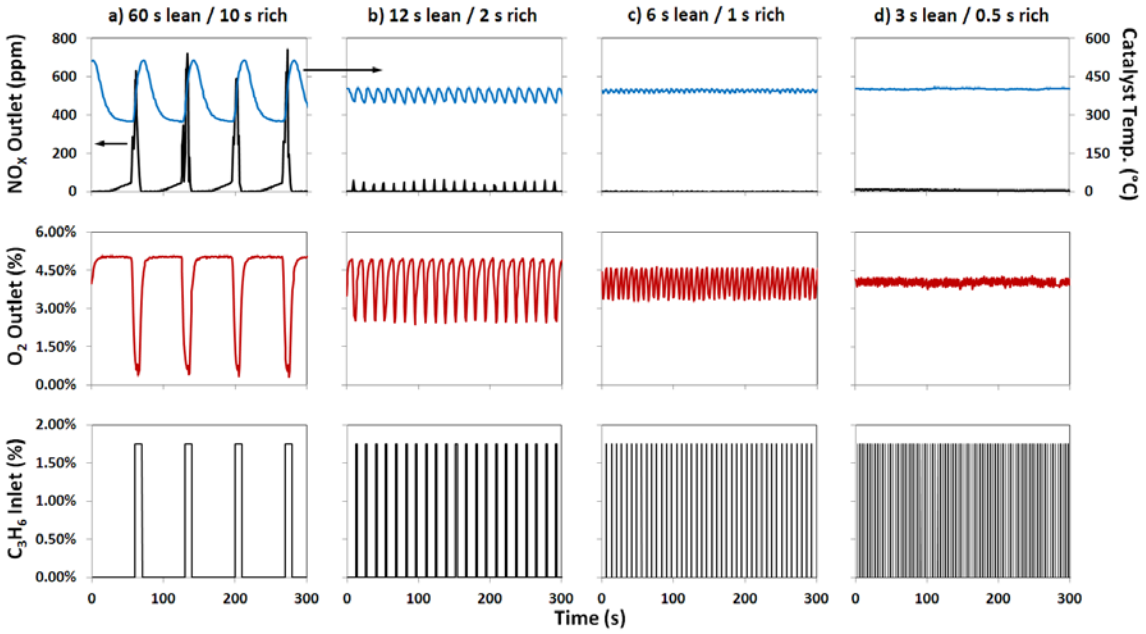

Fig. 2. Effluent NO_x/O_2 concentration and catalyst temperature for a set of typical cycling experiments, with the corresponding propylene injection patterns shown in the bottom row of the figure. Rich duty cycle and C_3H_6 concentration during the rich pulse are fixed at 14.3% and 1.75%, respectively. Feed stream contains 5% O_2 and 500 ppm NO at 275°C. Injection patterns for each column are as follows: a) 60 s lean/10 s rich (0.014 Hz). b) 12 s lean/2 s rich (0.07 Hz). c) 6 s lean/1 s rich (0.14 Hz). d) 3 s lean/0.5 s rich (0.29 Hz).

lean/0.5 s rich (0.29 Hz). The feed gas contained 500 pm NO and 5% O_2 in balance N_2 at a feed temperature of 275°C. During the rich phase, the concentration of C_3H_6 was 1.75%, corresponding to a rich pulse stoichiometric number ($S_{N,p}$) of 0.64 and a cycle-averaged value (S_N) of 4.5. The cycle-averaged C_3H_6 feed concentration was fixed for all four experiments.

The longer cycle time results in Fig. 2 have features similar to those reported and explained in previous studies that employed an aerobic regeneration [6,7,10,23]. The features include the gradual breakthrough of NO_x during the lean phase followed by a sharp NO_x spike at the beginning of the rich phase, which is accompanied by a sharp dip in the O_2 effluent concentration and a notable temperature rise during the rich phase. It is now generally established that NO_x is stored on the barium sites of the catalyst in the form of barium nitrates and nitrites during the lean phase [7,8,11]. Unreacted “slip” of NO_x in the form of NO and NO_2 occurs during the lean phase as the storage sites become occupied, resulting in a gradual increase in the effluent NO_x concentration. In order to avoid a large breakthrough of NO_x, the C_3H_6 reductant is injected during the rich phase to regenerate the storage sites through the reduction of surface nitrates/nitrites. The sharp spike in NO_x concentration is attributed to a shift in the gas phase composition that enabled NO_x storage and the generation of NO as the surface barium nitrates decompose, which can occur at temperatures above 400°C [31]. The catalytic oxidation of C_3H_6 results in a temperature increase, causing NO to be released more quickly than it can be converted to N_2 and leading to the NO_x puff in the effluent gas stream. A sustained feed of O_2 flow throughout the entire cycle (5%) is the cause of the appreciable exotherm.

Upon the stoppage of the reductant, the lean phase begins again, the temperature of the catalyst drops, and the cycle repeats.

As the cycle length was progressively shortened from 70 s to 3.5 s, a noted quantitative and qualitative change in the data was observed. The NO_x conversion obtained in the 0.29 Hz experiment (3 s lean/0.5 s rich) approached 100% compared to the ca. 90% value obtained for the 0.014 Hz experiment (60 s lean/10 s rich). Dramatic changes were also observed in the catalyst temperature transients. Higher frequency operation resulted in much less abrupt thermal swings than was encountered for the longer cycle lengths. The difference between the maximum and minimum temperatures decreased as the durations of the rich and lean phases were shortened, resulting in a steadier catalyst temperature. This result suggests an inability of the catalyst to respond thermally to the rapidly cycling feed conditions. The smaller variations in temperature were accompanied by a similar shift in the transient effluent O_2 concentration.

Few NO_x storage and reduction studies have appeared in which cycle times shorter than ca. 30 s have been used. Kabin et al. [10] reported a limiting conversion of 25% for a cycle time of 20 s, while Muncrief et al. [23] reported a decrease in the NO_x conversion below 40% for cycles less than 35 s. The low NO_x conversion was attributed to upstream mixing of the rich pulse and the adjacent lean phase gas due to dispersion in the tubing. Kabin et al. [10] also speculated that the catalyst response was too slow to respond to rapidly changing feed conditions associated with shorter cycle times, so that in effect the catalyst behaved as though the feed was mixed. More recently Shakya et al. [33] conducted experiments and developed a model for cycle times as short as 35 s.

The design of the reactor system in the current study was intended to minimize the upstream mixing of lean and rich streams. The positioning of the high speed injection valve in close proximity to the catalyst results in a smaller volume between the injection point and the catalyst, which reduces the time for upstream mixing. As a result, the catalyst encounters sharper lean-rich transitions and more rapid cyclic NO_x storage and reduction phases. Though it is not shown here, injection frequencies exceeding 0.5 Hz at the 14.3% rich duty cycle were found to achieve very low conversions in this system. At these conditions, the feed approaches that of a well-mixed feed as was encountered by Kabin et al. [10]. Additional factors may be inadequate radial mixing or a switching limitation of the injection valve. This warrants a study of alternative feed systems, but was not the focus of the current study.

3.2 Cycle-Averaged Performance Trends

3.2.1 Injection Frequency

Cycle-averaged effluent composition results provide further insight into the effect of pulse frequency. Fig. 3a and 3b show cycle-averaged effluent concentrations of the reactant and product species, while Fig. 3c and 3d show the corresponding cycle-averaged conversion, selectivities and catalyst temperature. The lean feed stream contained 800 ppm NO and 5% O_2 in balance N_2 at 260°C. The rich phase consisted of 2.03% C_3H_6, with the cycle-averaged S_N fixed at 3.9. The rich duty cycle was again fixed at 14.3%.

The data in Fig. 3 reveal decreasing effluent NO and NO_2 concentrations with increasing pulse frequency, consistent with the trends shown in Fig. 2 (i.e., increasing

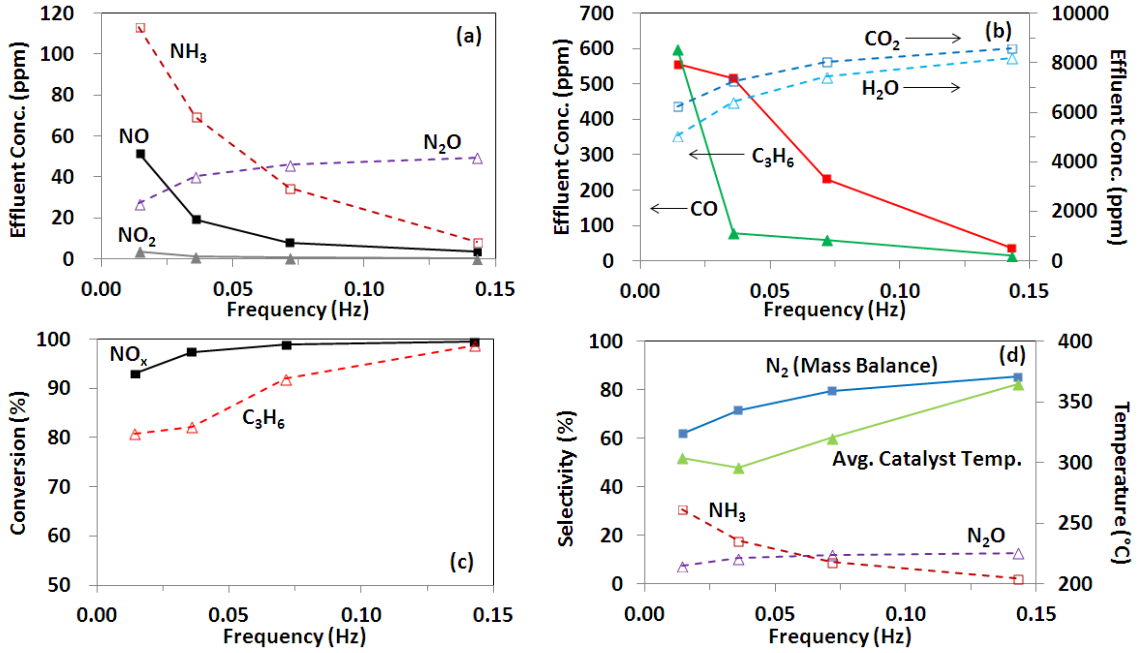

Fig. 3. Cycle-averaged concentrations as a function of injection frequency. Feed temperature is 260°C. Flow composition is 5% O_2 and 800 ppm NO. Rich phase C_3H_6 is 2.03% (S_N = 3.9). The injection frequencies are 0.014 Hz, 0.036 Hz, 0.07 Hz and 0.14 Hz. a) Cycle-averaged NO, NO_2, N_2O and NH_3 concentrations in the effluent stream. b) Cycle-averaged C_3H_6, CO, CO_2 and H_2O concentrations in the effluent stream. c) NO_x and C_3H_6 conversion data. d) N_2, N_2O and NH_3 selectivity with cycle-averaged catalyst temperature.

NO_x conversion with increasing frequency). The effluent concentrations of NH_3, CO and C_3H_6 also decreased with increasing injection frequency, while CO_2 and H_2O increased. The corresponding cycle-averaged NO_x and C_3H_6 conversions (Fig. 3c) show that near-complete conversion for both reactants is achieved for a frequency approaching 0.15 Hz.

The higher NO_x conversion achieved with the shorter cycle lengths indicates better utilization of the C_3H_6 reductant. Shorter rich cycles avoid prolonged oxygen deficient conditions in which O_2 is not available and C_3H_6 breakthrough occurs. The resulting higher C_3H_6 conversion is undoubtedly due to an increased extent of oxidation, evidenced by the higher production of CO_2 and H_2O and the higher cycle-averaged catalyst temperature (Fig. 3d). The higher temperature results in a higher N_2 selectivity

due to the increased rate of N-O bond scission and N adatom recombination [34]. Moreover, the reduction of NO_x to N_2 over the Pt sites is more favorable at higher temperatures [14].

The cycle-averaged results in Fig. 3a and 3b reveal a higher yield of NH_3 and CO during longer cycle time operation. The longer cycle times lead to oxygen deficient conditions, which expectedly lead to products of incomplete oxidation (CO) and NO_x reduction (NH_3). The generation of CO may also result in the production of H_2 via the water gas shift (WGS) reaction. H_2 that is produced from the WGS reaction readily reacts with adsorbed NO that forms during the regeneration phase, producing NH_3 [28]. In contrast, higher injection frequencies sustain gas phase O_2 at a higher level, avoiding the pronounced oxygen deficient conditions encountered at longer cycle times. As a result, more oxygen is available throughout the entire length of the cycle for the complete combustion of C_3H_6 to produce CO_2 and H_2O. This results in lower CO and NH_3 selectivities. The presence of more O_2 may also enhance the storage performance of the catalyst and result in less NO_x breakthrough during the lean phase, since O_2 is known to have a strong impact on the NO_x trapping process [6]. Furthermore, more O_2 at higher frequencies leads to a slight increase in N_2O selectivity, while N_2 selectivity increases due to the higher temperature (Fig. 3d).

The data in Fig. 2 and 3 showed that an appreciable exotherm results from the injection of propylene into the feed gas mixture and that faster injection results in a higher cycle-averaged catalyst temperature. In order to determine if this increased catalyst temperature is the sole factor in the conversion enhancement, an experiment was conducted at nearly constant catalyst temperature over a range of injection frequencies.

Fig. 4 shows the dependence of the cycle-averaged NO_x and propylene conversions on the pulse injection frequency. Similar to the previous experiments, the rich duty cycle and cycle-averaged amount of propylene injected were fixed. However, the feed temperature required to achieve the same cycle-averaged catalyst temperature at each frequency was determined through an iterative process, and the oven temperature was adjusted accordingly. Specifically, a cycle-averaged catalyst temperature of 410^{o}C (± 10^{o}C) was maintained for each frequency. The data show a similar trend to previous experiments, with a modest increase in the NO_x and propylene conversions as the injection frequency was increased. These findings suggest that the enhancement is not just a result of nonisothermal effects, but also involves a change in mechanism with the faster operation.

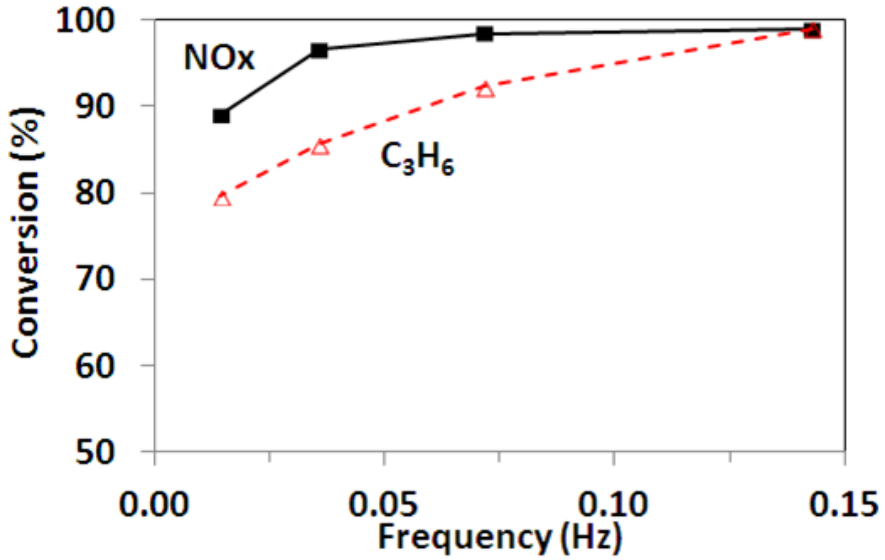

Fig. 4. NO_x and C_3H_6 conversion as a function of injection frequency at constant cycle-averaged catalyst temperature. Flow composition is 5% O_2, 10% CO_2 and 700 ppm NO. The rich phase C_3H_6 concentration is 1.9%. The feed temperature is adjusted to maintain a near constant-averaged catalyst temperature of 410°C ± 10°C. The injection frequencies are 0.014 Hz, 0.036 Hz, 0.07 Hz and 0.14 Hz.

It is instructive to determine if the fast cycling giving higher NO_x conversion and N_2 selectivity is robust to changes in the operating conditions. Fig. 5 shows the effect of pulse frequency for different cycle-averaged reductant concentrations. This experiment helps determine the minimum amount of reductant that must be injected to achieve a prescribed NO_x conversion. In this set of experiments, the cycle-averaged concentration

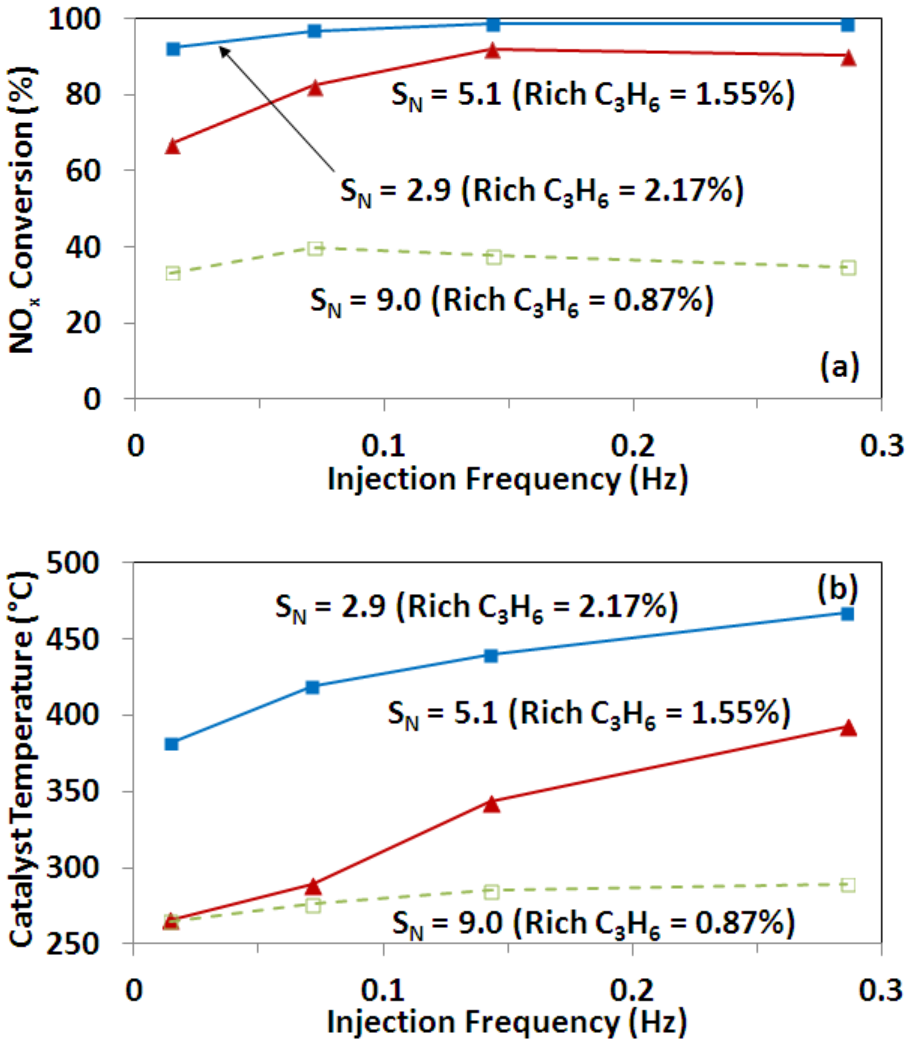

Fig. 5. NO_x conversion and catalyst temperature as a function of injection frequency, for three cycle-averaged C_3H_6 feed concentrations. Feed temperature is 275°C. Flow composition is 5% O_2 and 500 ppm NO. The injection frequencies are 0.014 Hz, 0.07 Hz, 0.14 Hz and 0.29 Hz. a) Cycle-averaged NO_x conversion as a function of injection frequency. b) Cycle-averaged catalyst temperature as a function of injection frequency.

was adjusted by varying the rich phase concentration of propylene between 2.17% and 0.87%, corresponding to S_N values between 2.9 and 9.0, respectively. All other conditions were the same as in Fig. 2; i.e. 500 ppm NO, 5% O_2 and balance N_2 at 275°C. The ratio of lean phase length to rich phase length was held at 6:1, corresponding to a rich duty cycle of 14.3%.

The NO_x conversion decreased as the cycle-averaged C_3H_6 feed concentration was decreased for all injection frequencies (Fig. 5a). This trend shows that less reductant leads to decreased NO_x conversion, an expected consequence of incomplete storage phase regeneration. Accompanying this trend was a decrease in the cycle-averaged temperature due to the lower propylene oxidation rate. Interestingly, for a feed with a cycle-averaged S_N = 5.1, a 90% NO_x conversion could be sustained with an injection frequency exceeding 0.15 Hz. In contrast, the conventional 60 s lean/10 s rich cycle timing gave a conversion of only ca. 65%.

For comparison, Fig. 6 shows the effect of injection frequency using H_2 as the reductant for the same frequencies and a similar range of S_N. In this set of experiments the feed contained 650 ppm NO and 3% O_2 at 275°C. The rich phase H_2 concentration was varied between 6.0% and 9.5%, corresponding to S_N values between 4.5 and 7.1, respectively. As previously noted, the NO_x conversion decreases as the cycle-averaged reductant concentration decreases due to incomplete storage phase regeneration. However, in contrast to the results of Fig. 5a in which C_3H_6 was the reductant, increasing the injection frequency resulted in a lower NO_x conversion when using H_2 as the

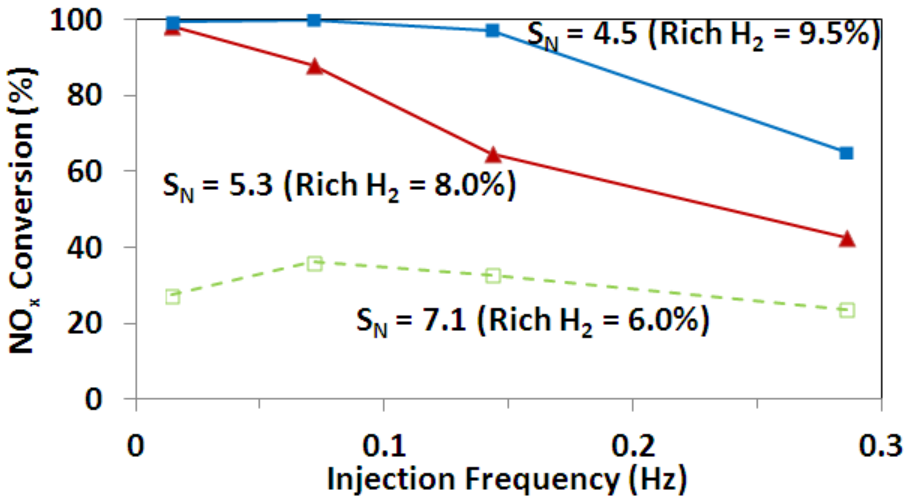

Fig. 6. NO_x conversion as a function of injection frequency, for three cycle-averaged H_2 feed concentrations. Feed temperature is 275°C. Flow composition is 3% O_2 and 650 ppm NO. The injection frequencies are 0.014 Hz, 0.07 Hz, 0.14 Hz and 0.29 Hz.

reductant. This suggests that the observed performance enhancement when using C_3H_6 is not simply a result of the injection system, since the same trend is not observed when using H_2.

3.2.2 Thermal Durability

Another important exhaust parameter is the feed temperature. Fig. 7 compares the cycle-averaged NO_x conversions as a function of the feed temperature for two different cycle times (60 s lean/10 s rich and 6 s lean/1 s rich) corresponding to pulse frequencies of 0.014 and 0.14 Hz, respectively. The feed stream contained 700 ppm NO and 5% O_2 in balance N_2, and the rich phase contained 1.75% C_3H_6. The corresponding catalyst temperature is provided on the right vertical axis of Fig. 7. The NO_x conversion shows the characteristic maximum as a function of feed temperature in each of the cases. NO_x conversion is limited by C_3H_6 light-off (which occurs at ca. 210 °C) at low temperatures and the thermal stability of barium nitrates/nitrites at high temperatures.

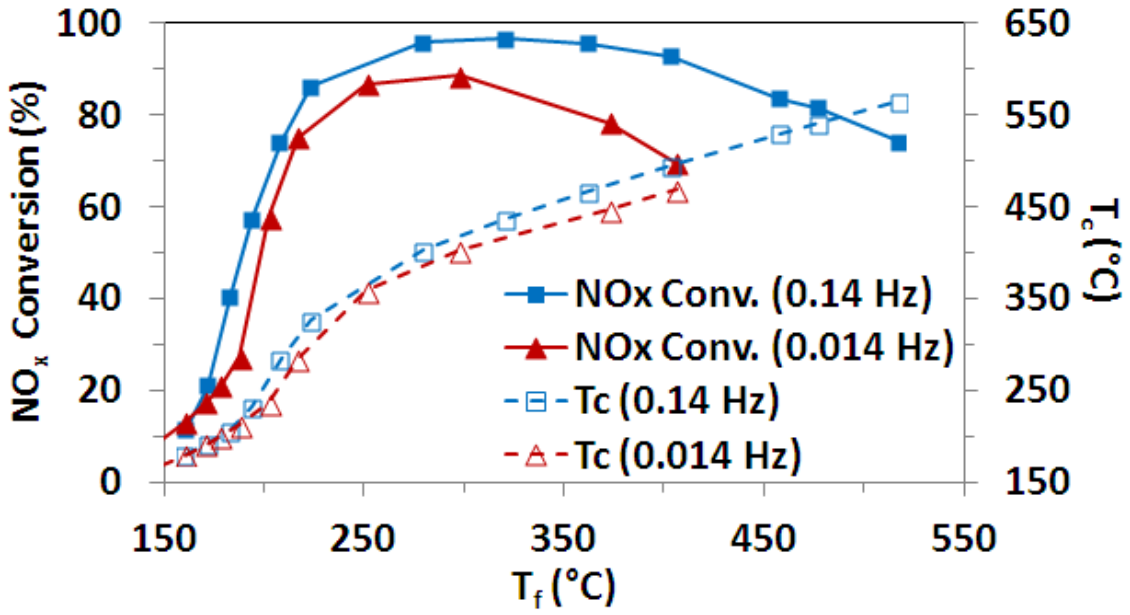

Fig. 7. Cycle-averaged NO_x conversion and catalyst temperature vs. feed temperature for two different frequencies. Flow composition is 5% O_2 and 700 ppm NO. The rich phase contains 1.75% C_3H_6. The injection patterns are 6 s lean/1 s rich (0.14 Hz) and 60 s lean / 10 s rich (0.014 Hz).

Notably, the higher frequency resulted in enhanced NO_x conversion over the entire range of feed temperatures. These findings are consistent with those reported by Inoue et al. [30]. That is, rapid propylene pulsing just upstream of the catalyst clearly gives better results over a wide range of temperatures. On the other hand, Bisaiji et al. [29] reported that at low temperatures, longer cycle times gave higher NO_x conversion than shorter cycle times. This disparity in the low temperature trends is not easily resolved since the reductant was not specifically identified by the authors for the conversion versus temperature data. Moreover, differences in catalyst formulation and operating conditions could result in a decreased binding strength for intermediates on the catalyst surface, leading to lower thermal stability.

3.2.3 Rich Phase Composition

Another experiment was conducted to determine if the reductant feed concentration during rapid injection plays a role in the NO_x conversion enhancement. Kabin et al. [10] showed during conventional NSR operation that higher NO_x conversion was obtained if propylene was injected in short, concentrated bursts as opposed to longer, less concentrated pulses. To examine the generality of this trend for fast cycling, a series of experiments were conducted in which the rich phase propylene concentration was varied over a moderate range of values while the total amount of propylene fed was held constant. Rather than adjusting the rich duty cycle to sustain a fixed amount of propylene injected, the C_3H_6 concentration in the lean phase was compensated to maintain a constant cycle-averaged C_3H_6 feed concentration in the lean regime (S_N = 3.9). This approach allowed the injection frequency to be fixed. The feed temperature was 250°C, and the lean feed mixture contained 550 ppm NO, 5% O_2 and balance N_2. The cycle timings considered were 60 s lean/10 s rich (0.014 Hz) (Fig. 8a) and 6 s lean/1 s rich (0.14 Hz) (Fig. 8b).

The Fig. 8 data show that more concentrated rich pulses resulted in enhanced NO_x conversion for both injection frequencies. A sharp decrease in the NO_x conversion was observed at an intermediate rich phase C_3H_6 concentration of 1.25% and 1.75% for the 70 s and 7 s cycle lengths, respectively. A similar conversion trend was reported in the aforementioned study of Kabin et al. [10] who used a 49 s total cycle length with a varying rich duty cycle. Kabin et al. [10] attributed the drop in conversion to dispersion induced dilution of the less concentrated rich pulses with the lean phase. They showed that the resulting conversion approached that obtained for a steady-state feed having the

same cycle-averaged feed composition. For the current data, the shift in the concentration at which the drop in NO_x conversion occurs is attributed to upstream dispersion, which is magnified at the higher injection frequencies.

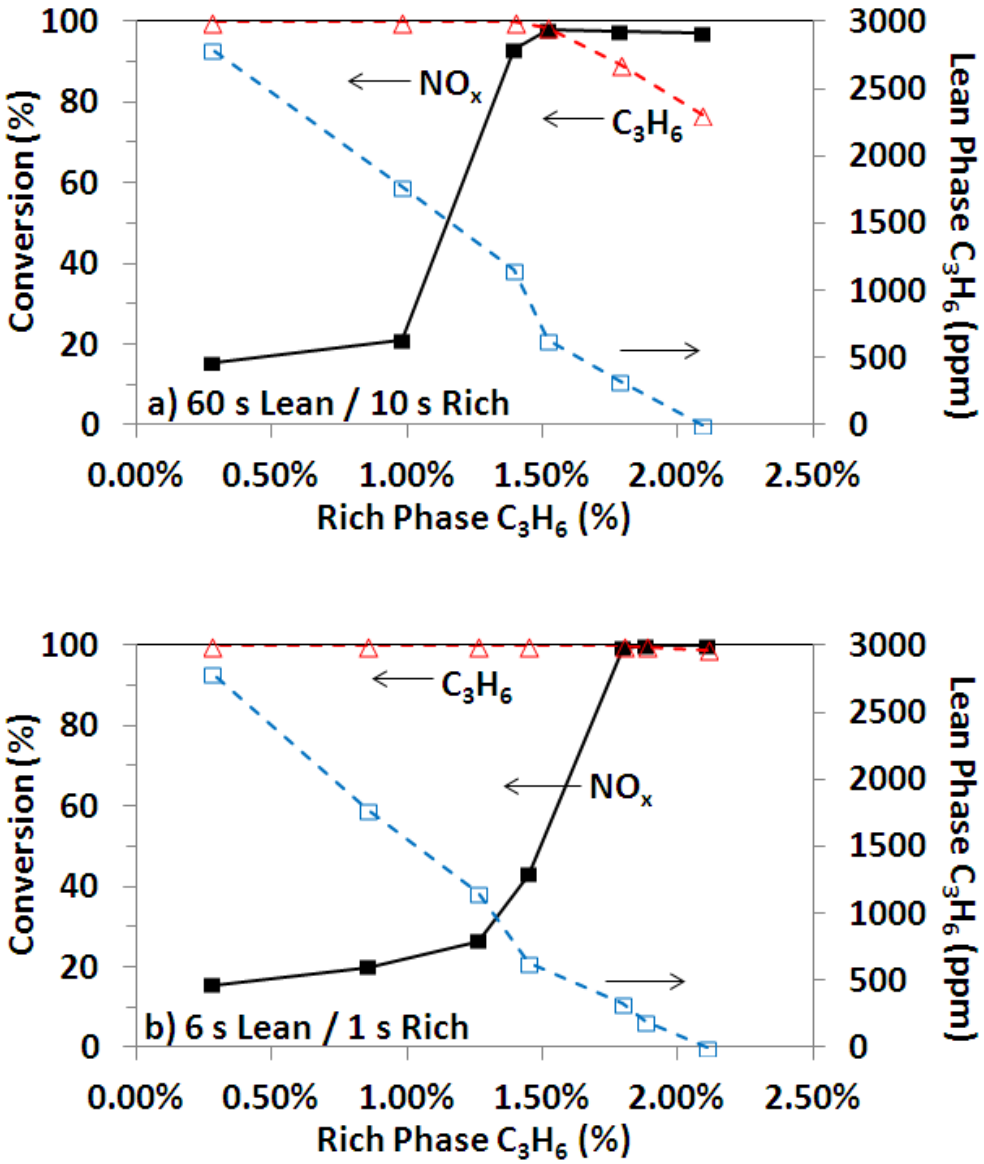

Fig. 8. Cycled-averaged NO_x and C_3H_6 conversions verses rich phase propylene feed concentration. Lean phase C_3H_6 concentration is adjusted to maintain a cycle-averaged C_3H_6 concentration of 0.29% (S_N=3.9). Feed temperature is 250°C. Flow composition is 5% O_2 and 550 ppm NO. a) Conversions using a 60 s lean / 10 s rich (0.014 Hz) cycling pattern. b) Conversions using a 6 s lean / 1 s rich (0.14 Hz) cycling pattern.

The data also reveal a trade-off between high NO_x conversion and high C_3H_6 conversion for the 0.014 Hz injection pattern (Fig. 8a). While more concentrated rich pulses resulted in higher NO_x conversion, an appreciable amount of C_3H_6 breakthrough occurred. In contrast, at the higher 0.14 Hz injection frequency (Fig. 8b), high conversions for both NO_x and C_3H_6 were obtained when the rich pulse was sufficiently concentrated. As discussed earlier, the maintenance of a moderate O_2 concentration level throughout the entire cycle results in higher propylene conversion.

3.2.4 Lean Phase Duration

Additional tuning of the operating conditions to achieve high NO_x and propylene conversions with high N_2 selectivity could involve the adjustment of the lean phase duration phase. A set of experiments were conducted in which the duration of the lean phase was systematically varied over a wide range while fixing the duration of the rich pulse. The feed stream contained 600 ppm NO, 5% O_2 and balance N_2 at a feed temperature of 300°C. The rich phase duration and C_3H_6 rich feed concentration were maintained at 0.5 s and 1.9%, respectively.

Effluent concentrations of the reacting species are shown in Fig. 9a and 9b, while the corresponding conversion and selectivity data are provided in Fig. 9c and 9d, respectively. Fig. 9c also reports the cycle-averaged S_N over the range of lean phase durations. The NO_x conversion decreases monotonically with an increase in the lean phase duration (Fig. 9c). A longer lean phase is expectedly less effective in trapping the NO_x due to the filling of storage sites and the insufficient amount of reductant to regenerate the catalyst [10]. A sharp increase in the effluent concentration of NO_x was observed at a lean duration of 4 s, corresponding to $S_N = 6$. Notably, this conversion drop

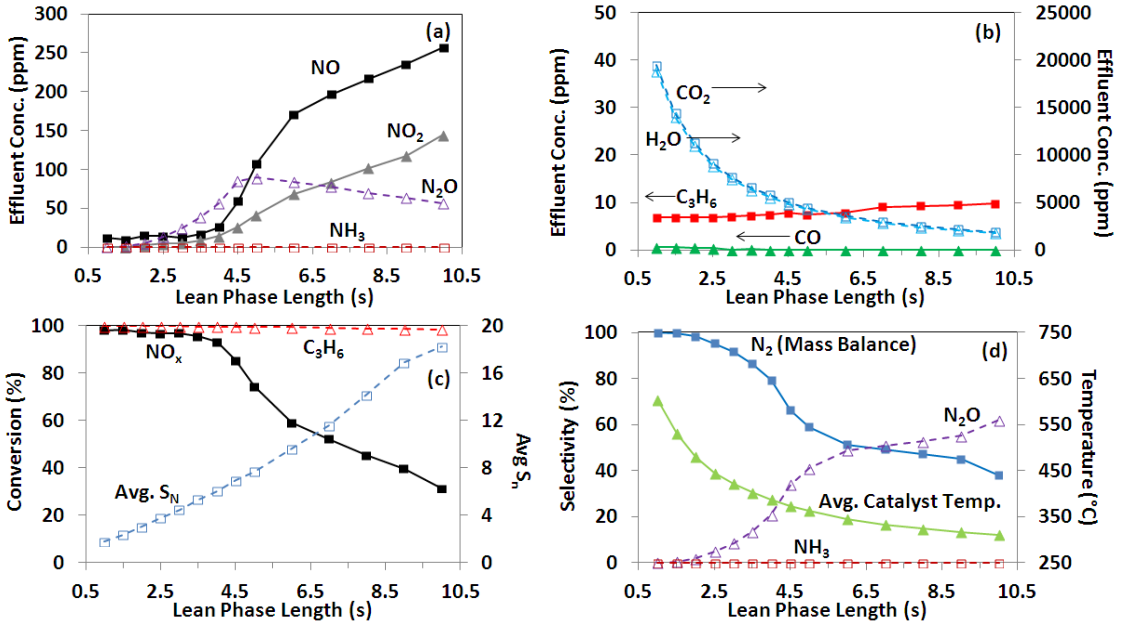

Fig. 9. Cycle-averaged concentrations as a function of lean phase length. Feed temperature is 300°C. Flow composition is 5% O_2 and 600 ppm NO. Rich phase C_3H_6 is 1.9% ($S_{N,p}$ = 0.6) and rich pulse duration is 0.5 s. Total cycle length and S_N varies. a) Cycle-averaged NO, NO_2, N_2O and NH_3 concentrations in the effluent stream. b) Cycle-averaged C_3H_6, CO, CO_2 and H_2O concentrations in the effluent stream. c) NO_x and C_3H_6 conversion data with corresponding average S_N. d) N_2, N_2O and NH_3 selectivity with cycled-averaged catalyst temperature.

occurred at a higher S_N than previous literature values using conventional cycle timing. For example, Kabin et al. [10] achieved >90% conversion for a cycle-averaged stoichiometric number as high as 3.9 using a 60 s lean/10 s rich cycle pattern under similar feed conditions. Thus, less propylene was required using rapid injection to achieve a high NO_x conversion.

In contrast to NO_x conversion, the propylene conversion is high over the entire range of lean phase durations (Fig. 9c). Increased lean phase duration decreases the cycle-averaged C_3H_6 concentration, resulting in a lower cycle-averaged catalyst temperature. The concentrations of CO_2/H_2O drop accordingly (Fig. 9b). The decrease in catalyst temperature is also accompanied by a decrease in the cycle-averaged N_2

selectivity and increase in the N_2O selectivity. A maximum effluent concentration of N_2O is achieved at a lean phase duration of 5 s (Fig. 9a). To the left of this maximum, the temperature is too high for N_2O to survive; to the right of the maximum the lower conversion of NO_x means a lower N_2O yield, although the selectivity increases moderately. The effluent concentrations of CO and NH_3 were negligible for the entire range of lean phase durations.

3.2.5 Impact of CO_2

The effect of CO_2 may provide some insight into the underlying mechanism of rapid injection NSR. CO_2 is an important constituent in exhaust gas, so it is of interest to determine its effect during fast cycling NSR. As mentioned earlier, previous studies have generally shown that CO_2 is detrimental to NSR performance [24,41–43]. This is due primarily to the higher stability of barium carbonates, which are detrimental to the dynamic NO_x storage. The Toyota Di-Air papers included CO_2 in their study [29,30], but its effect was not specifically studied.

The effect of CO_2 on the cycle-averaged NO_x conversion as a function of injection frequency is shown in Fig. 10. In these experiments, the feed stream contained 550 ppm NO, 5% O_2, and either 0% or 10% CO_2 in balance N_2. The rich phase C_3H_6 concentration was 2.2%, while the feed temperature was either 250°C (Fig. 10a) or 375°C (Fig. 10b). For all injection frequencies and both feed temperatures, the presence of CO_2 had a negative effect on the NO_x conversion, an expected result. The decrease in NO_x conversion in the presence of 10% CO_2 was somewhat larger at 250°C than at 375°C. Fig. 10c reports the percent decrease in the NO_x conversion at the four injection frequencies and two temperatures. As stated, decreases were observed in all cases.

However, and interestingly, the effect of CO_2 was less detrimental when higher propylene injection frequency was used.

One explanation for the effect of temperature and injection frequency on the extent of CO_2 inhibition concerns the storage process. The dynamic storage capacity is smaller at 250°C than at 375°C [23], so the formation of carbonate species rather than nitrates at the Ba sites has a greater impact, and more NO_x slip occurs during the lean phase at the lower temperature. In addition, the effect of CO_2 is lessened as the injection frequency is increased for both temperatures. This can be attributed to the decreased barium utilization at higher frequencies, since less storage is required for short cycle lengths. This diminishes the impact of carbonate formation on NO_x conversion.

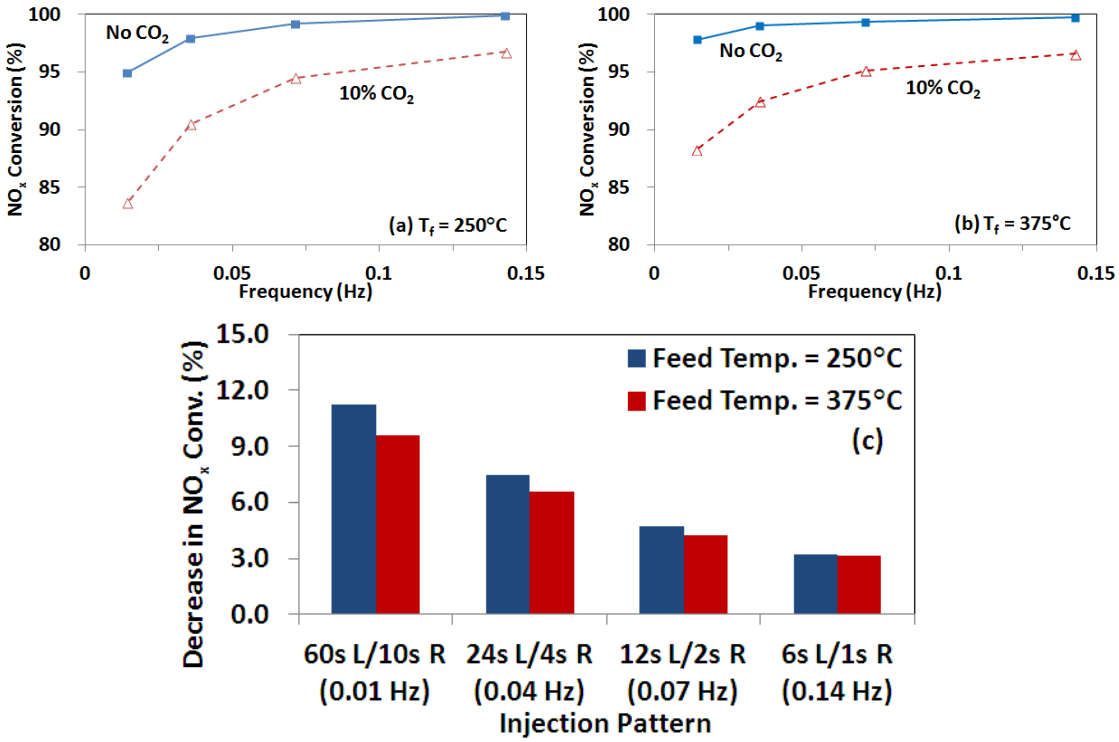

Fig. 10. Effect of CO_2 on NO_x conversion for varying frequencies. Flow composition is 5% O_2, 550 ppm NO, and 0% (—■—) or 10% (—▲—) CO_2. Rich phase C_3H_6 is 2.2%. a) NO_x conversion at T_f = 250°C. b) NO_x conversion at T_f = 375°C. c) Decrease in NO_x conversion due to the addition of 10% CO_2 at T_f = 250°C and T_f = 375°C.

3.3 Transient Approach to Cyclic Steady State

The results shown so far reveal the clear advantage of rapid pulsing in terms of cycle-averaged NO_x conversion and N_2 selectivity. In order to understand the mechanistic implications of these findings, some features of the transient behavior are worth examining. As is known in vehicular emission catalysis, the transient performance of the converter is critical, especially during the so-called “cold-start” phase. Emissions of pollutants during the cold start dominate the overall emissions in conventional urban driving. In addition, changes in the engine load during typical start/stop driving translate into dynamical changes in the exhaust gas temperature, flowrate, and composition. Finally, from a fundamental mechanistic standpoint, transient behavior can provide important clues about the underlying reaction pathways and kinetics.

In the Toyota study [29], pertinent observations were reported about the transient features of the Di-Air process. In a particular experiment at 340°C feed temperature, a 98% cycle-averaged NO_x conversion was achieved for a feed containing about 55 ppm NO_x. While this performance is impressive, a long transient in the approach to the cyclic steady state of ca. 100 s was reported. During this transient, a large amount of unreacted NO_x escaped the reactor. The authors did not elaborate on this feature in any detail, but this would appear to be an important factor for the reasons outlined above.

Here we report some findings to investigate whether such transient behavior is characteristic of fast cycling NSR, and if so, understand how it provides information about the underlying mechanism. In this experiment, we followed the transient approach to cyclic steady state for a range of injection frequencies. Fig. 11 shows the instantaneous NO_x released during the transient startup of lean-rich cycling over a catalyst with

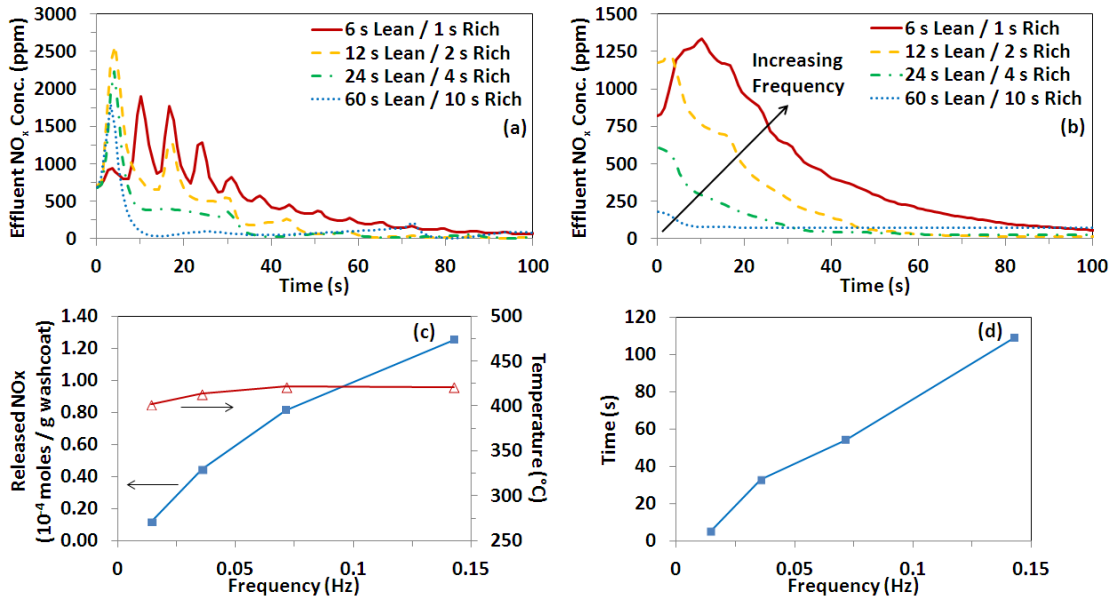

Fig. 11: Transient NO_x released in the effluent as the reactor transitions from lean conditions with NO_x initially stored on the catalyst to periodic steady state cycling conditions. Feed composition is 5% O_2, 10% CO_2, 700 ppm NO and rich phase C_3H_6 = 1.9%. The feed temperature is adjusted to maintain a near constant cycle-averaged catalyst temperature (Avg. T_c = 410°C ± 10°C). Cycling begins at t=0 s. a) Transient NO_x concentration. b) Moving average of transient NO_x concentration, averaged over 1 cycle length. c) Moles of NO_x released in the effluent and average catalyst temperature. d) Time required for NO_x averaged over 1 cycle to reach 95% of the periodic steady state cycle-averaged NO_x concentration value.

pre-stored NO_x. The feed composition was 800 ppm NO, 5% O_2, 10% CO_2, and balance N_2. The rich phase C_3H_6 concentration was 1.9%. Prior to the pulsed injection of propylene, the lean gas mixture was fed over the catalyst for 45 min to allow for the storage of NO_x. Then lean-rich cycling commenced (as indicated in Fig. 11) at 0 s. In order to reduce the temperature effect on NO_x storage capacity, the feed temperature was adjusted to maintain a nearly constant steady state T_c (cycle-averaged T_c = 410°C ± 10°C) using the method discussed earlier. Although not shown here, similar results were observed without adjusting the feed temperature.

Fig. 11a shows the transient NO_x released for 100 s from the start of cycling for several different injection frequencies. Fig. 11b shows the corresponding moving average gas species concentrations (over one full cycle) to smooth-out the data. The transient data show an interesting NO_x release versus time dependence. For each injection frequency, the effluent NO_x exhibited a maximum value from the initial 800 ppm, and eventually approached the cyclic steady state value. More importantly, the higher frequencies, while achieving an overall higher cycle-averaged steady state NO_x conversion, resulted in a higher averaged peak NO_x value and required more time to reach the cyclic steady state.

An analysis of the effluent NO_x during the transition from storage to steady state cycling indicated that more NO_x was released in higher frequency operation. Fig. 11c shows the total amount of NO_x released during the transition to steady state cycling. Fig. 11d reports the amount of time required for the moving average NO_x concentration to reach 95% of the steady state value. Both the total NO_x released and the time to reach steady state monotonically increase with the injection frequency. Similarly, the catalyst temperature (not shown here) increases more gradually at higher frequencies and also requires more time to reach steady state. A discussion of the phenomenological mechanism for these data follows.

3.4 Phenomenological Mechanism

The data presented for rapid injection NSR collectively provide a body of observations that help to unravel the underlying mechanism. The pioneering works by Toyota provided reactor data and surface IR measurements that suggest the formation of reactive intermediates including R-NO_x, R-ONO, R-CH=NOH, and R-C=ONH_2 as a result of the production of reactive precursors in the form of oxygenates during rapid

cycling [29]. The intermediates are then converted selectively through reaction with surface and gas phase NO_x species to N_2. Here we assess data reported in the current study in terms of the mechanism proposed by Toyota.

During conventional NSR operation with typical cycle timing and injection frequencies on the order of 0.01 Hz, the NO_x conversion is largely dependent on the storage properties of the catalyst. The prevailing understanding of conventional NSR is that spillover processes play an important role in both the storage of NO_x and its regeneration [8]. NO_x stored in the proximity of the precious metal crystallites is more efficiently converted due to shorter diffusion distances [6,35–40]. Therefore, stored nitrites and nitrates in the proximity of the precious metal crystallites are crucial for eventual reduction to N_2 during the regeneration phase. The process works well in a window of temperatures, ca. 200 – 400°C. At higher temperatures, the diminished storage capacity due to barium nitrate decomposition leads to higher NO_x breakthrough during the storage phase. As a result, a drop in NO_x conversion is observed above 400°C.

In contrast, the data of the Toyota researchers, corroborated in the current study, show that high reductant injection frequencies reduces the importance of storage capacity and barium nitrate decomposition becomes a less dominant process. The primary limitation at high temperatures becomes the decomposition of formed hydrocarbon intermediates that reduce NO_x, which may not have to be stored NO_x. Since this process occurs at a higher temperature than barium nitrate decomposition, the high NO_x conversion temperature range is extended. The data reported in the current study appear to support the reaction mechanism proposed by Bisaiji et al. [29] and Inoue et al. [30].

The slow transient approach to the cyclic steady state (Fig. 11) supports the mechanism proposed by Inoue et al. [30] that a reactive intermediate accumulates on the catalyst surface. At the high injection frequency, the reductant C_3H_6 is only able to react with surface nitrates stored in close proximity to Pt sites. That is, due to the short duration of the rich phase, only the "proximal" stored NO_x is able to diffuse to the sites and react before the next cycle begins. As the temperature gradually increases due to the oxidation of C_3H_6, nitrates on barium sites that are kinetically inaccessible begin to decompose. This leads to increased NO_x released.

Moreover, higher frequencies result in more moderate O_2 concentrations throughout the cycle length. The sustained presence of O_2 may make nitrate decomposition less likely from a thermodynamic standpoint and could facilitate NO_x trapping through the oxidation of NO to NO_2 [6]. Another potential consequence of high frequency injection is that it may be more difficult for C_3H_6 to scavenge oxygen adsorbed on the Pt crystallites down the entire length of the catalyst due to the short rich phases. One of the functions of the reductant is to react with adsorbed oxygen in order to free-up Pt sites for NO_x reduction to occur [6,23]. Shorter rich cycles may require more time to reach oxygen species adsorbed down the entire length of the monolithic catalyst, in contrast to lengthy rich phases with excess C_3H_6 provided. As a result, more time (multiple regenerations) would be needed to approach the cyclic steady state.

Chapter 4. Conclusions

A study of the rapid injection of C_3H_6 using a high speed switching valve in close proximity to a NSR catalyst was conducted. The effects of injection speed, feed temperature, rich phase composition, lean phase length, and the presence of CO_2 on NO_x conversion were determined.

In contrast to traditional NSR cycling systems involving H_2 as the reductant, NO_x conversion increased with increasing injection frequency. The shorter cycle times resulted in a steadier rate of exothermic catalytic oxidation of C_3H_6, evidenced by pseudo steady state values for the catalyst temperature and O_2 concentration. The reduced cycle duration allowed a higher conversion of C_3H_6 to be obtained throughout the length of the cycle. As shown by the comparison to H_2 experiments, the change in performance for C_3H_6 was not solely the result of the modified injection system; rather, the results are indicative of a qualitative mechanistic change. An increased temperature range for high NO_x conversion was obtained, due to the diminished role of NO_x storage. The decomposition of $Ba(NO_3)_2$, which occurs above 400°C, was found not to be the limiting factor at high injection frequencies. Instead, the hydrocarbon intermediates which remain up to 600°C are likely the overriding factor, allowing an extension of the high conversion temperature range. Also, similar to traditional NSR cycling, more concentrated rich pulses were found to achieve a higher NO_x conversion than rich pulses of reduced concentration. However, in contrast to the traditional injection pattern, high conversions of both NO_x and C_3H_6 were obtained for sufficiently concentrated rich pulses at the 0.14 Hz injection frequency. Through the variation of cycle length, less reductant was required to achieve high NO_x conversion (>90% for $S_N = 6$). In addition, the inhibitory effect of

$BaCO_3$ formation was determined to be less detrimental at high injection frequencies due to low utilization of dynamic storage sites. Lastly, increased injection frequencies were observed to require a longer time to reach pseudo steady state values and released more adsorbed NO_x during the transition period. This may be attributed to diffusion limitations at short cycle lengths of NO_x not stored in close proximity to Pt sites or a moving reductant front that requires more time to scavenge oxygen adsorbed on Pt sites down the length of the catalyst. These results are consistent with hydrocarbon intermediates on the catalyst surface providing competition for the C_3H_6 oxidation reaction and reducing NO_x.

The temperature range observed in this study is somewhat smaller than that observed in the Toyota works, which reported NO_x conversion of 80% at catalyst temperatures of nearly 700°C [32]. In the current study, a NO_x conversion of 80% was obtained at catalyst temperatures as high as 550°C. However, the catalyst composition and the reductant used in the study were not specified. Moreover, a significantly lower NO feed concentration was used. Thus, a different hydrocarbon may have produced a more thermally stable surface intermediate, leading to greater NO_x conversion at high temperatures.

Chapter 5. Future Work

5.1 Process Optimization

Further research will need to be conducted in order to gain better insight into the properties and mechanism of the Di-Air phenomenon. Since the entry length of the reactor was found to be an important process variable, computational fluid dynamics (CFD) can be used to model the fluid mechanics of the reactor upstream of the catalyst to identify the ideal entry length of this system. This will help minimize axial dispersion in the reactor upstream, while ensuring proper radial dispersion to all channels of the monolith. Additionally, future experiments can be performed in order to study the effect of the injection pattern. Since optimized values for a traditional NSR system have been adopted for the majority of this study, the impact of different rich duty cycles may be worth investigation.

5.2 Reaction Mechanism

Several experiments can be conducted to help elucidate the reaction mechanism for the process. In terms of the mechanism developed by Bisaiji et al. [32], the reduction of NO_x by intermediates is proposed to occur in two generalized reactions: the reaction between partially oxidized hydrocarbons and adsorbed NO_x to form the surface intermediates, and the subsequent reaction between the intermediates and NO_x to form N_2. The following experiments can be performed to gather information required to develop a more detailed mechanism.

Due to the inherent spatial gradient along the length of monolith catalysts and the transient nature of NSR operation, the use of a spatially resolved capillary inlet mass

spectrometer (SpaciMS) can provide detailed concentration and temperature profiles otherwise unattainable. The SpaciMS can be used to obtain spatial and temporal concentration profiles down the length of the catalyst with minimal disruption to the system through the use of movable capillaries inserted into the monolith channels. The partially oxidized hydrocarbons that react to form the intermediates are thought to form in the front portion of the catalyst, leading to the generation of intermediates on the catalyst downstream. Assuming these partially oxidized hydrocarbons exist in the gas phase, the SpaciMS should enable their identification and the conditions necessary for their production (air to fuel ratio, temperature, etc.). Alternatively, if this instrument is not available, a shorter length of catalyst can be cut and the outlet can be measured with FTIR or GCMS. Though this will not provide spatial resolution, it may still allow the identification of the partially oxidized hydrocarbons.

The characterization of surface intermediates can be obtained by producing partially oxidized HCs over a short length of catalyst and sending it to a powdered NSR catalyst to be analyzed using *in-situ* DRIFTS. Toyota noted that the intermediates are formed over an NSR catalyst, but not over a DOC catalyst [32]. The characteristics of NSR catalysts that enable this phenomenon can be studied by testing the effect of catalyst composition on the formation of the intermediate surface species. Since stored NO_x has been suggested to take part in the formation of the intermediates, the presence of Ba is expected to be essential. The formation of the intermediates likely occurs over Pt or possibly at the Pt-Ba interface as stored nitrates move to Pt, and the intermediates may bind to either component. Studying the effect of Pt loading and dispersion on the generation of intermediates may not only be noteworthy for the development of a more

detailed mechanistic picture, but also for the determination of the economic viability of the process. For example, if a lower composition of the precious metal function is sufficient for the formation of the surface intermediates, then the precious metal loading in the front portion can be higher (for the oxidation reaction) while the back portion can have a lower loading (making the catalyst cheaper). In addition, the impact of Ce may also be worth examining, since the effect of oxygen storage on the process is unclear.

Once the partially oxidized hydrocarbons are identified, it may also be worthwhile to attempt the generation of the surface intermediates directly from cylinder gas of these compounds. If feasible, this could isolate the effect of the individual gas components for a multi-component mixture and help determine if there are any other factors that are significant to achieving the formation of the intermediates that cannot be separated when using rapid hydrocarbon injection (e.g., oscillating O_2 concentration). This would also, in effect, turn the inherently transient nature of cyclic NSR operation into a steady state reaction and simplify the development of a reaction mechanism.

5.3 Development of a Model

A temporal analysis of products (TAP) reactor can potentially be used to measure the kinetics of the reaction between the intermediates and NO_x. Since the reactor is operated in high vacuum, external mass transfer limitations are absent. Thus, the chemical reaction rate can be isolated from the physical transport rate. By using an Ar carrier gas, the rate of formation of N_2 could be found using a mass spectrometer.

Furthermore, the use of temperature programmed desorption (TPD) can provide the desorption characteristics of the intermediates. This technique can be used to find the surface coverage of species, the desorption order, and the desorption energy through

iterative calculations once the order is determined. This information can be used in the formation of a model.

Once a better fundamental understanding of the reactions is obtained, a Microkinetic model can be developed. A reaction mechanism can be proposed for the generation of the intermediates and the reduction of NO_x based on the previous experiments. Assumptions for the mechanism (Langmuir-Hinshelwood vs. Eley-Rideal, rate determining step, etc.) will need to be determined as more experimental data is acquired. Required thermodynamic properties can be obtained through databases, experimental results and estimation.

In the long term, this study can be extended to higher molecular weight hydrocarbons. Different hydrocarbons may produce intermediates with different adsorption characteristics and potentially different properties. The switch from a gas phase to a liquid phase reductant would require modification of the reactor design to achieve vaporization and adequate mixing. Since the application of this technology in vehicles would likely use diesel fuel as the reductant for practical purposes, experimentation using diesel fuel is desired for more accurate modeling of a realistic engine system.

References

[1] DieselNet, Emission Standards – United States, Cars and Light-Duty Trucks – Tier 2, http://www.dieselnet.com/standards/us/ld_t2.php (2013).

[2] DieselNet, Emission Standards – European Union, Cars and Light Trucks, http://www.dieselnet.com/standards/eu/ld.php (2013).

[3] N. Miyoshi, S. Matsumoto, K. Katoh, T. Tanaka, J. Hardara, N. Takashi, K. Yokota, M. Sugiura, K. Kasahara, "Development of New Concept Three-Way Catalyst for Automotive Lean-Burn Engines," *SAE Technical Paper Series* 950809 (1995).

[4] N. Takahashi, H. Shinjoh, T. Iijima, T. Suzuki, K. Yamazaki, K. Yokota, H. Suzuki, N. Miyoshi, S.I. Matsumoto, T. Tanizawa, T. Tanaka, S.S. Tateishi, K. Kasahara, "The new concept 3-way catalyst for automotive lean-burn engine: NO_x storage and reduction catalyst," *Catal. Today* 27 (1996) 63.

[5] W. Bogner, M. Kramer, B. Krutzsch, S. Pischinger, D. Voigtlander, G. Wenninger, F. Wirbeleit, M.S. Brogan, R.J. Brisley, D.E. Webster, "Removal of nitrogen oxides from the exhaust of a lean-tune gasoline engine," *Appl. Catal. B Environ.* 7 (1995) 153.

[6] W.S. Epling, L.E. Campbell, A. Yezerets, N.W. Currier, J.E. Parks, "Overview of the Fundamental Reactions and Degradation Mechanisms of NO_x Storage/Reduction Catalysts," *Catalysis Reviews: Science and Engineering* 46:2 (2004) 163-245.

[7] S. Roy, A. Baiker, "NO_x Storage−Reduction Catalysis: From Mechanism and Materials Properties to Storage−Reduction Performance," *Chem. Rev.* 109 (2009) 4054-4091.

[8] M.P. Harold, "NO_x storage and reduction in lean burn vehicle emission control: a catalytic engineer's playground," *Current Opinion in Chemical Engineering* (2012) 1:303-311.

[9] R.D. Clayton, M.P. Harold, V. Balakotaiah, "NO_x storage and reduction with H_2 on $Pt/BaO/Al_2O_3$ monolith: Spatio-temporal resolution of product distribution," *Appl. Catal. B* 84 (2008) 616-630.

[10] K. Kabin, R. Muncrief, M.P. Harold, "NO_x storage and reduction on a Pt/BaO/alumina monolithic storage catalyst," *Catal. Today* 96 (2004) 79-89.

[11] L. Lietti, P. Forzatti, I. Nova, E. Tronconi, "NO_x Storage Reduction over Pt Ba/γ-Al_2O_3 Catalyst," *Journal of Catalysis* 204 (2001) 175-191.

[12] P. Jozsa, E. Jobson, M. Larsson, "Reduction of NO_x stored at low temperatures on a NO_x adsorbing catalyst," *Topics in Catalysis* 30-31 (2004) 177-180.

[13] J.R. Theis, J.A. Ura, J.J. Li, G.G. Surnilla, J.M. Roth, C.T. Goralski, "NO_x Release Characteristics of Lean NO_x Traps During Rich Purges," *SAE Int.* 2003-01-1159, 5 (2003).

[14] I. Nova, L. Castoldi, L. Lietti, E. Tronconi, P. Forzatti, "On the dynamic behavior of NO_x-storage/reduction $Pt–Ba/Al_2O_3$ catalyst," *Catal. Today* 75 (2002) 431.

[15] W.P. Partridge, J.-S. Choi, "NH3 formation and utilization in regeneration of $Pt/Ba/Al_2O_3$ NO_x storage-reduction catalyst with H_2," *Applied Catalysis B: Environmental* 91 (2009) 144-151.

[16] I. Nova, L. Lietti, P. Forzatti, "Mechanistic aspects of the reduction of stored NO_x over $Pt–Ba/Al_2O_3$ lean NO_x trap systems," *Catalysis Today* 136 (2008) 128-135

[17] L. Cumaranatunge, S.S. Mulla, A. Yezerets, N.W. Currier, W.N. Delgass, F.H. Ribeiro, "Ammonia is a hydrogen carrier in the regeneration of $Pt/BaO/Al_2O_3$ NO_x traps with H_2," *Journal of Catalysis* 246 (2007) 29–34.

[18] S.S. Mulla, S.S. Chaugule, A. Yezerets, N.W. Currier, W.N. Delgass, F.H. Ribeiro, "Regeneration mechanism of $Pt/BaO/Al_2O_3$ lean NO_x trap catalyst with H_2," *Catalysis Today* 136 (2008) 136-145.

[19] R.D. Clayton, M.P. Harold, V. Balakotaiah, "Selective catalytic reduction of NO by H_2 in O_2 on $Pt/BaO/Al_2O_3$ monolith NO_x storage catalysts," *Applied Catalysis. B* 81 (2008) 161-181.

[20] J.A. Pihl, J.E. Parks, C. Stuart Daw, T.W. Root, "Product Selectivity During Regeneration of Lean NO_x Trap Catalysts," *SAE Tech. Paper* 2006-01-3441, 2006.

[21] R.D. Clayton, M.P. Harold, V. Balakotaiah, "NO_x storage and reduction with H_2 on $Pt/BaO/Al_2O_3$ monolith: Spatio-temporal resolution of product distribution," *Applied Catalysis B: Environmental* 84 (2008) 616-630.

[22] J. Xu, R. Clayton, V. Balakotaiah, M.P. Harold, "Experimental and microkinetic modeling of steady-state NO reduction by H_2 on $Pt/BaO/Al_2O_3$ monolith catalysts," *Applied Catalysis B: Environmental* 77 (2008) 395-408.

[23] R. Muncrief, K. Kabin, M.P. Harold, "NO_x Storage and Reduction with Propylene on Pt/BaO/Alumina," *AIChE Journal* Vol. 50, No. 10 (2004).

[24] W.S. Epling, J.E. Parks, G.C. Campbell, A. Yezerets, N.W. Currier, L.E. Campbell, "Further evidence of multiple NO_x sorption sites on NO_x storage/reduction catalysts," *Catal. Today* 96 (2004) 21-30.

[25] V.G. Easterling, Y. Ji, M. Crocker, M. Dearth, R.W. McCabe, "Application of spaciMS to the study of ammonia formation in lean NO_x trap catalysts," *Applied Catalysis B: Environmental* 123-124 (2012) 339-350.

[26] J.-S. Choi, W.P. Partridge, W.S. Epling, N.W. Currier, T.M. Yonushonis, "Intra-channel evolution of carbon monoxide and its implication on the regeneration of a monolithic $Pt/K/Al_2O_3$ NO_x," *Catalysis Today* 114 (2006) 102-111.

[27] J.P. Breen, R. Burch, C. Fontaine-Gautrelet, C. Hardacre, C. Rioche, "Insight into the key aspects of the regeneration process in the NO_x storage reduction (NSR) reaction probed using fast transient kinetics coupled with isotopically labelled ^{15}NO over Pt and Rh-containing Ba/Al_2O_3 catalysts," *Appl. Catal. B* 81 (2008) 150.

[28] P. Dasari, R. Muncrief, M.P. Harold, "Cyclic Lean Reduction of NO by CO in Excess H_2O on $Pt–Rh/Ba/Al_2O_3$: Elucidating Mechanistic Features and Catalyst Performance," *Topics in Catalysis* (2013) 1-15.

[29] Y. Bisaiji, K. Yoshida, M. Inoue, K. Umemoto, T. Fukuma, "Development of Di-Air - A New Diesel $deNO_x$ System by Adsorbed Intermediate Reductants," *SAE Int. J. Fuels Lubr.* 5 (2012) 380-388.

[30] M. Inoue, Y. Bisaiji, K. Yoshida, N. Takagi, T. Fukuma, "$deNO_x$ Performance and Reaction Mechanism of the Di-Air System," *Topics in Catal.* 56 (2013) 3-6.

[31] E. Fridell, M. Skoglundh, B. Westerberg, S. Johansson, G. Smedler, "NO_x Storage in Barium-Containing Catalysts," *Journal of Catal.* 183 (1999), 196.

[32] G. Zhou, T. Luo, R.J. Gorte, "An investigation of NO_x storage on $Pt–BaO–Al_2O_3$," *Applied Catalysis B: Environmental* 64 (2006) 88-95.

[33] B.M. Shakya, M.P. Harold, V. Balakotaiah, "Effect of cycle time on NH_3 generation on low Pt dispersion $Pt/BaO/Al_2O_3$ catalysts: Experiments and crystallite-scale modeling," *Chem. Engineering Journal* 230 (2013) 584-594.

[34] J. Xu., M.P. Harold, V. Balakotaiah, "Microkinetic modeling of steady-state $NO/H_2/O_2$ on $Pt/BaO/Al_2O_3$ NOx storage and reduction monolith catalysts," *Appl. Catal. B* 89 (2009) 73-86.

[35] R.D. Clayton, M.P. Harold, V. Balakotaiah, "Performance Features of Pt/BaO Lean NO_x Trap with Hydrogen as Reductant," *AIChE Journal*, Vol. 55, No. 3 (2009).

[36] N.W. Cant, I.O.Y. Liu, M.J. Patterson, "The effect of proximity between Pt and BaO on uptake, release, and reduction of NO_x on storage catalysts," *Journal of Catalysis* 243 (2006) 309-317.

[37] R. Büchel, R. Ströbel, A. Baiker, S.E. Pratsinis, "Effect of the Proximity of Pt to Ce or Ba in $Pt/Ba/CeO_2$ Catalysts on NO x Storage–Reduction Performance," *Topics in Catalysis* 52 (2009) 1709-1712.

[38] H. Mahzoul, J.F. Brilhac, P. Gilot, "Experimental and mechanistic study of NO_x adsorption over NO_x trap catalysts," *Applied Catalysis B: Environmental* 20 (1999) 47-55.

[39] E.C. Corbos, X. Courtois, F. Can, P. Marécot, D. Duprez, "NO_x storage properties of Pt/Ba/Al model catalysts prepared by different methods: Beneficial effects of a N_2 pre-treatment before hydrothermal aging," *Applied Catalysis B: Environmental* 84 (2008) 514-523.

[40] J. Hepburn, E Thanasiu, D. Dobson, W. Watkins, "Experimental and Modeling Investigations of NO_x Trap Performance," *SAE Technical Paper* 962051 (1996) 71.

[41] Y. Ren, M.P. Harold, "NO_x Storage and Reduction with H_2 on Pt/Rh/BaO/CeO_2: Effects of Rh and CeO_2 in the Absence and Presence of CO_2 and H_2O," *ACS Catal.* 1 (2011) 969-988.

[42] F. Basile, A. Gambatesa, G. Fornasari, M. Livi, A. Vaccari, "CO_2 effect on activity and stability of NO_x storage reduction catalysts," *Topics in Catalysis* 42-43 (2007) 165-169.

[43] F. Rodrigues, L. Juste, C. Potvin, J.F. Tempère, G. Blanchard, G. Djéga-Mariadassou, "NO_x storage on barium-containing three-way catalyst in the presence of CO_2," *Catalysis Letters* 72 (2001) 59-64.